Pergamon

Acta mater. Vol. 45, No. 10, pp. 4271–4281, 1997
© 1997 Acta Metallurgica Inc.
Published by Elsevier Science Ltd. All rights reserved
Printed in Great Britain
PII: S1359-6454(97)00080-3
1359-6454/97 $17.00 + 0.00

PREDICTION OF MICROSTRUCTURE IN MONOCLINIC $LaNbO_4$ BY ENERGY MINIMIZATION

LI JIAN and RICHARD D. JAMES

Department of Aerospace Engineering & Mechanics, University of Minnesota, 110 Union St. SE, Minneapolis, MN 55455, U.S.A.

(Received 13 January 1997)

Abstract—The continuum theory developed by Ball and James has been applied to predict the microstructure in $LaNbO_4$, such as morphology of domains, domain boundary, and crystallographic relationship between domains. The results from the theory are in good agreement with that from direct examination by transmission electron microscopy (TEM) and optical microscopy. © *1997 Acta Metallurgica Inc.*

1. INTRODUCTION

Based on non-linear thermoelasticity, Ball and James [1] have developed a theory of martensite microstructures. This theory has been successfully applied to several shape memory alloys [2–4], predicting the morphology of martensite, orientation relationship between austenite and martensite, habit planes, as well as twinning relationship between martensites.

The basic assumptions of the theory are as follows: (1) the atomic scale free energy per unit volume is only a function of lattice vectors and temperature. Once the temperature and the atomic position on the Bravais lattice are specified, the free energy density is known. (2) The free energy is defined for lattice vectors belonging to the "Ericksen–Pitteri neighborhood". In particular this implies that the point group symmetry of the martensitic phase is a subgroup of that of the parent phase. (3) The lattice vectors of the parent and martensitic phases are assumed to minimize the lattice scale free energy. (4) The passage from atomic lattice to continuum theory is based on the Born rule, which states that deformations $\mathbf{y}:\Omega \to \mathbb{R}^3$ (Ω is the reference configuration) of a crystal viewed as a continuum are related to atomic scale lattice deformations described by a deformation of the lattice vectors $\mathbf{e}_i \to \mathbf{F}\mathbf{e}_i$, $i = 1, 2, 3$, according to the formula

$$\nabla \mathbf{y}(\mathbf{x}) = \mathbf{F} \tag{1}$$

where the deformation gradient $\nabla \mathbf{y}(\mathbf{x})$ and $\mathbf{F}$ are 3×3 matrices. The total free energy E of the body is assumed to have the form

$$E = \int_\Omega W(\nabla \mathbf{y}(\mathbf{x}), T)\, d\mathbf{x} \tag{2}$$

where T is the temperature, under the condition that no external forces are applied to the body. By minimizing the total free energy,

$$\min \int_\Omega W(\nabla \mathbf{y}(\mathbf{x}), T)\, d\mathbf{x} \tag{3}$$

the microstructure can be predicted.

$LaNbO_4$, a ferroelastic material, has two polymorphs. The low temperature phase, crystallized in the monoclinic scheelite structure, has point group 2/m. The high temperature phase belongs to tetragonal scheelite structure with a point group 4/m. The phase transformation occurs near 520°C. Although the transformation has been identified to be a second order transition and therefore not a martensitic transformation by the usual convention [5, 6], the assumptions on which the theory has been developed are still good ones for this type of ferroelastic phase transition.

The purpose of the present paper is to apply the Ball–James theory to the ferroelastic transition in $LaNbO_4$ and to analyze the microstructure in the low temperature monoclinic phase, predicting the domain structure, such as the location of the domain boundary, the crystallographic orientation relationship between domains and the interface between a domain laminate and a single domain. These results are compared with the experimental evidence of Li and Wayman [5–7]. For several of the calculations done in Section 2, we are pleased to acknowledge the related calculations done by Chu [8].

In this paper $\mathbf{a} \wedge \mathbf{b}$ denotes the cross product between two vectors $\mathbf{a}$ and $\mathbf{b}$, $\mathbf{a} \otimes \mathbf{b}$ denotes the matrix with the property that $(\mathbf{a} \otimes \mathbf{b})\mathbf{x} = \mathbf{a}(\mathbf{b} \cdot \mathbf{x})$ for all vectors $\mathbf{x}$ and vectors are generally small bold Latin letters while matrices are capital bold Latin letters.

2. THEORETICAL APPROACH

Since the transformation in $LaNbO_4$ is a second order transition, there is no temperature range in which the parent tetragonal phase and the product monoclinic phase coexist. The reference configuration is chosen as the tetragonal lattice at the transition temperature T_c, and the deformed configuration then is the monoclinic lattice at any temperature below T_c. As mentioned above, the transition belongs to the type 4/mF2/m, the symbol representing a transition from the prototype with a point group 4/m to the ferroelastic phase with a point group 2/m [9], leading to the loss of a four-fold rotation symmetry element. According to Ball–James theory, two orientation states of domain are expected. Let $\mathbf{U}_1$ and $\mathbf{U}_2$ represent the lattice deformations which map the tetragonal lattice vectors $\{\mathbf{e}_1^t, \mathbf{e}_2^t, \mathbf{e}_3^t\}$ to two sets of particular monoclinic lattice vectors $\{\mathbf{e}_1^{m_1}, \mathbf{e}_2^{m_1}, \mathbf{e}_3^{m_1}\}$ and $\{\mathbf{e}_1^{m_2}, \mathbf{e}_2^{m_2}, \mathbf{e}_3^{m_2}\}$, respectively, i.e.

$$\mathbf{e}_i^{m_1} = \mathbf{U}_1\mathbf{e}_i^t \tag{4a}$$

$$\mathbf{e}_i^{m_2} = \mathbf{U}_2\mathbf{e}_i^t \quad i = 1, 2, 3 \tag{4b}$$

$\mathbf{U}_1$, $\mathbf{U}_2$ are related by the lost 90° rotation $\mathbf{R}_s$ about the $\mathbf{e}_2^t$ axis, i.e.

$$\mathbf{U}_2 = \mathbf{R}_s\mathbf{U}_1\mathbf{R}_s^T \tag{5}$$

where the superscript T denotes the transpose of the matrix, and

$$\mathbf{R}_s = \begin{bmatrix} 0 & 0 & 1 \\ 0 & 1 & 0 \\ -1 & 0 & 0 \end{bmatrix}$$

in the tetragonal basis. According to the polar decomposition, it is always possible to assume that $\mathbf{U}_1$ and $\mathbf{U}_2$ are symmetric matrices with all their eigenvalues larger than zero.

Based on assumption (4), if we take the deformation gradients as $\mathbf{U}_1$ and $\mathbf{U}_2$, the energy density W reaches the minimum. It is also understood that any rigid rotation of the deformed lattice does not change the free energy of the lattice. This means that for any rotation matrices $\mathbf{R}_1$ and $\mathbf{R}_2$, $\mathbf{R}_1\mathbf{U}_1$ and $\mathbf{R}_2\mathbf{U}_2$ have the same value of W as $\mathbf{U}_1$ and $\mathbf{U}_2$. Adopting the circle-dot notation of energy wells [2], the energy wells represented by $\mathbf{R}_1\mathbf{U}_1$ and $\mathbf{R}_2\mathbf{U}_2$ are shown in Fig. 1. The basic assumption of the Ball–James theory is that $W(\mathbf{F}, \theta)$ is minimized as long as $\mathbf{F}$ belongs to the two circles.

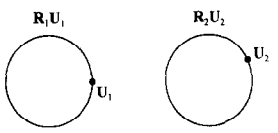

Fig. 1. Schematic diagram showing the energy wells. Each circle represents the set of matrices of the form $\mathbf{RA}$, where $\mathbf{R}$ is a rotation matrix and $\mathbf{A} = \mathbf{U}_1$ or $\mathbf{U}_2$.

2.1. Prediction of the domain boundary

Let us consider a deformation $\mathbf{y}(\mathbf{x})$ of the form $\nabla\mathbf{y}(\mathbf{x}) = \mathbf{R}_1\mathbf{U}_1$ for $\mathbf{x}\cdot\mathbf{n} \leqslant 0$ and $\nabla\mathbf{y}(\mathbf{x}) = \mathbf{R}_2\mathbf{U}_2$ for $\mathbf{x}\cdot\mathbf{n} \geqslant 0$. When the equation

$$\mathbf{R}_2\mathbf{U}_2 - \mathbf{R}_1\mathbf{U}_1 = \mathbf{a}' \otimes \mathbf{n}, \tag{6}$$

where $\mathbf{a}' \otimes \mathbf{n}$ represents the tensor product of vectors $\mathbf{a}'$ and $\mathbf{n}$, is satisfied, the deformation at the domain boundary $\mathbf{x}\cdot\mathbf{n} = 0$ is continuous. By solving equation (6), the crystallographic index of the domain boundary can be predicted.

Left-multiplying both sides of equation (6) by the inverse of $\mathbf{R}_1$, we get

$$\mathbf{R}\mathbf{U}_2 - \mathbf{U}_1 = \mathbf{a} \otimes \mathbf{n} \tag{7}$$

where $\mathbf{R} = \mathbf{R}_1^{-1}\mathbf{R}_2$, $\mathbf{a} = \mathbf{R}_1^{-1}\mathbf{a}'$. Right-multiplied by $\mathbf{U}_1^{-1}$ and rearranged, equation (7) becomes

$$\mathbf{R}\mathbf{U}_2\mathbf{U}_1^{-1} = \mathbf{I} + \mathbf{a} \otimes \mathbf{n}'$$

where $\mathbf{n}' = \mathbf{U}_1^{-1}\mathbf{n}$.

Let $\mathbf{A} = \mathbf{R}\mathbf{U}_2\mathbf{U}_1^{-1}$, $\mathbf{C} = \mathbf{A}^T\mathbf{A}$, then

$$\mathbf{C} = (\mathbf{R}\mathbf{U}_2\mathbf{U}_1^{-1})^T(\mathbf{R}\mathbf{U}_2\mathbf{U}_1^{-1}) = (\mathbf{I} + \mathbf{a} \otimes \mathbf{n}')^T(\mathbf{I} + \mathbf{a} \otimes \mathbf{n}')$$

i.e.

$$\mathbf{C} = \mathbf{U}_1^{-1}\mathbf{U}_2^2\mathbf{U}_1^{-1} = (\mathbf{I} + \mathbf{n}' \otimes \mathbf{a})(\mathbf{I} + \mathbf{a} \otimes \mathbf{n}'). \tag{8}$$

Given $\mathbf{U}_1$, $\mathbf{U}_2$, there are solutions of $(\mathbf{a}, \mathbf{n}')$ of equation (8) if and only if the middle eigenvalue of $\mathbf{C}$ is 1 (see Ref. [1]). Generally, there are two sets of solutions (corresponding to $\kappa = \pm 1$ below) satisfying $\det(\mathbf{I} + \mathbf{a} \otimes \mathbf{n}') > 0$ and these are given by

$$\mathbf{n}' = \rho\left(\sqrt{\frac{\lambda_3(1-\lambda_1)}{\lambda_3-\lambda_1}}\,\mathbf{e}_1 + \kappa\sqrt{\frac{\lambda_1(\lambda_3-1)}{\lambda_3-\lambda_1}}\,\mathbf{e}_3\right) \tag{9}$$

$$\mathbf{a} = \rho^{-1}\left(\frac{\sqrt{\lambda_3}-\sqrt{\lambda_1}}{\sqrt{\lambda_3-\lambda_1}}\right)\left(-\sqrt{1-\lambda_1}\,\mathbf{e}_1 + \kappa\sqrt{\lambda_3-1}\,\mathbf{e}_3\right) \tag{10}$$

where $\rho(\neq 0)$ is a constant, and $\mathbf{e}_1$, $\mathbf{e}_3$ are normalized eigenvectors of $\mathbf{C}$ corresponding to eigenvalues λ_1, λ_3, respectively ($0 < \lambda_1 \leqslant \lambda_2 = 1 \leqslant \lambda_3$). $\mathbf{R}$ can be obtained from

$$\mathbf{R} = (\mathbf{U}_1 + \mathbf{a} \otimes \mathbf{n})\mathbf{U}_2^{-1}. \tag{11}$$

For convenience, we choose the origin $\mathbf{x} = 0$ on the boundary between two domains. Applying equation (7) to any vector $\mathbf{x}$ on the boundary, we have

$$\mathbf{R}\mathbf{U}_2\mathbf{x} - \mathbf{U}_1\mathbf{x} = (\mathbf{a} \otimes \mathbf{n})\mathbf{x} = \mathbf{a}(\mathbf{n}\cdot\mathbf{x}). \tag{12}$$

As required by the continuity of the deformation at the boundary,

$$\mathbf{R}\mathbf{U}_2\mathbf{x} = \mathbf{U}_1\mathbf{x}$$

so that from equation (12),

$$\mathbf{a}(\mathbf{n}\cdot\mathbf{x}) = 0. \tag{13}$$

Equation (13) indicates that vector $\mathbf{n}$ is perpendicular to any vectors lying on the boundary, so that $\mathbf{n}$ is the

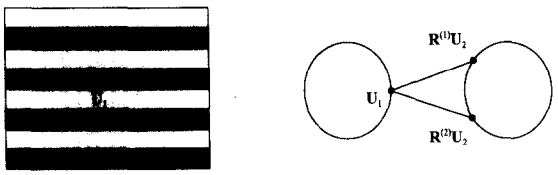

Fig. 2. Predicted domain laminate structure (a) and the corresponding energy well notation (b). In (b) a straight line connecting two matrices means that they differ by a matrix of rank one.

normal vector to the boundary plane in the reference configuration; $\mathbf{n}'$ $(=\mathbf{U}_1^{-1}\mathbf{n})$ is then the normal to the deformed boundary plane. Thus the boundary plane is determined, as well as the deformations on each side of the boundary. Figure 2(a) is a schematic picture of the predicted domain laminate structure of domains, and the energy well notation for two compatible solutions is shown in Fig. 2(b).

2.2. *Prediction of the orientation relationship between domains*

Equation (4) describes the lattice transformation between the parent lattice and the product lattice, respectively, without considering the compatibility of the two deformations in the product phase. For the particular deformation analyzed in Section 2.1, equation (4) should be expressed as

$$\mathbf{e}_i^{m_1} = \mathbf{U}_1\mathbf{e}_i^{I} \tag{14a}$$

$$\mathbf{e}_i^{m_2} = \mathbf{R}\mathbf{U}_2\mathbf{e}_i^{I}. \tag{14b}$$

Substituting equation (5) into (14b)

$$\mathbf{e}_i^{m_2} = \mathbf{R}\mathbf{R}_s\mathbf{U}_1\mathbf{R}_s^{T}\mathbf{e}_i^{I}, \quad i = 1, 2, 3. \tag{15}$$

As mentioned earlier, $\mathbf{R}_s$ is a symmetry operation of the parent lattice, and so is $\mathbf{R}_s^{T}$. Hence, by definition of the point group of a lattice, $\mathbf{R}_s^{T}\mathbf{e}_i^{I}$ can be expressed as linear combinations of $\mathbf{e}_j^{I}$, i.e.

$$\mathbf{R}_s^{T}\mathbf{e}_i^{I} = \mu_i^j\mathbf{e}_j^{I} \tag{16}$$

where all μ_i^j are integers, and $\det(\mu_i^j) = \pm 1$. Combining equations (15) and (16) we get

$$\mathbf{e}_i^{m_2} = \mathbf{R}\mathbf{R}_s\mathbf{U}_1\mu_i^j\mathbf{e}_j^{I} = \mathbf{R}\mathbf{R}_s\mu_i^j\mathbf{U}_1\mathbf{e}_j^{I} = \mathbf{R}\mathbf{R}_s\mu_i^j\mathbf{e}_j^{m_1}$$

or

$$\mu_j^i\mathbf{e}_i^{m_2} = \mathbf{R}\mathbf{R}_s\mathbf{e}_j^{m_1}. \tag{17}$$

With the choice of $\mathbf{R}_s$ given in equation (5) we find from equation (16) that

$$\mu_i^j = \begin{bmatrix} 0 & 0 & -1 \\ 0 & 1 & 0 \\ 1 & 0 & 0 \end{bmatrix}.$$

It is known that if $\{\mathbf{e}_i\}$ denotes lattice vectors for a certain Bravais lattice, then so do $\{\mu_i^j\mathbf{e}_j\}$ for any μ_i^j with properties given above. Hence, $\mu_j^i\mathbf{e}_i^{m_2}$ can also be recognized as another set of the monoclinic lattice vectors $\mathbf{e}_j^{II}$ representing the same monoclinic lattice as given by $\mathbf{e}_i^{m_2}$. Redesignating $\mathbf{e}_j^{m_1}$ as $\mathbf{e}_j^{I}$, from equation (17) we obtain the crystallographic relationship between the two compatible monoclinic lattices I and II as

$$\mathbf{e}_j^{II} = \mathbf{R}\mathbf{R}_s\mathbf{e}_j^{I}. \tag{18}$$

2.3. *Prediction of laminate/domain interface*

When two domain laminates meet each other, the simplest situation is that one laminate meets one of the domains in the other laminate, forming a laminate/domain interface such as shown schematically in Fig. 3(a). As proved by Ball and James, this interface is not exactly compatible, and an intermediate layer with a thickness of $1/k$ must be introduced, where k is an integer. Assuming that the deformation gradients in the laminate are $\nabla\mathbf{y} = \mathbf{U}_1/\mathbf{R}\mathbf{U}_2/\mathbf{U}_1/\mathbf{R}\mathbf{U}_2/\ldots$, then the average deformation gradient $\mathbf{C}_\lambda$ in the region of laminate is a linear combination of $\mathbf{U}_1$ and $\mathbf{R}\mathbf{U}_2$:

$$\mathbf{C}_\lambda = \lambda\mathbf{R}\mathbf{U}_2 + (1-\lambda)\mathbf{U}_1 \tag{19}$$

with $0 \leqslant \lambda \leqslant 1$, the volume fraction of domain 2 in the laminate. The deformation in the intermediate layer is compatible with both sides of the region. Even though the deformation gradients in the layer are away from the energy wells, the energy in the layer tends to zero as k approaches infinity, and the energy of the deformed body is minimized on the energy wells, if the following overall compatibility equation holds:

$$\mathbf{Q}_i\mathbf{C}_\lambda - \mathbf{U}_i = \mathbf{b}_i \otimes \mathbf{m}_i, \quad i = 1, 2 \tag{20}$$

corresponding to two domain orientations, respectively, where $\mathbf{Q}_i$ is a rotation matrix. It is easily verified that for each $\lambda \in (0, 1)$, the middle eigenvalue of $\mathbf{U}_i^{-1}\mathbf{C}_\lambda^{T}\mathbf{C}_\lambda\mathbf{U}_i^{-1}$ is 1. As above [cf. equations (9) and (10)] we expect two solutions for each value of $\lambda \in (0, 1)$. One of the two solutions is trivial for the laminate/single domain situation [8], and the other can be solved as follows.

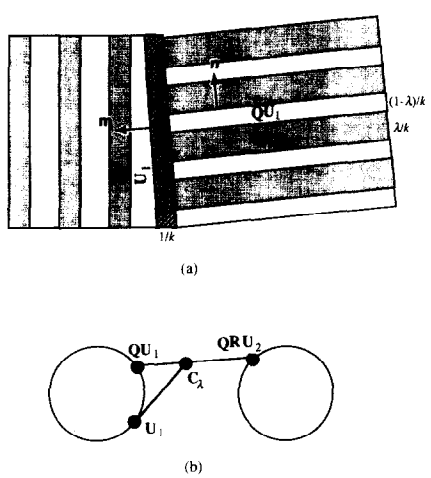

Fig. 3. Predicted laminate/domain structure (a) and its energy well notation (b).

Table 1. Dependence of lattice parameters on temperature in $LaNbO_4$

Temperature (°C)	c_1^m (Å)	c_2^m (Å)	c_3^m (Å)	β (degrees)
21	5.633	11.666	5.261	94.15
300	5.596	11.745	5.314	93.01
400	5.565	11.765	5.356	92.25
470	5.530	11.778	5.381	91.53
480	5.525	11.783	5.395	91.22
490	5.520	11.794	5.391	91.15
495	5.502	11.797	5.405	91.00
500	5.496	11.795	5.411	90.90
505	5.497	11.799	5.417	90.83
510	5.502	11.801	5.429	90.68
515	5.494	11.799	5.427	90.53
	c_1^t	c_2^t	c_3^t	
520	5.450	11.80	5.450	90.00

For the case of $\mathbf{Q}_1\mathbf{C}_i - \mathbf{U}_1 = \mathbf{b}_1 \otimes \mathbf{m}_1$, substituting equation (19), we have

$$\mathbf{Q}_1(\lambda\mathbf{R}\mathbf{U}_2 + (1-\lambda)\mathbf{U}_1) - \mathbf{U}_1 = \mathbf{b}_1 \otimes \mathbf{m}_1. \quad (21)$$

Substituting equation (7) into (21), we have

$$\mathbf{Q}_1(\mathbf{U}_1 + \lambda\mathbf{a} \otimes \mathbf{n}) - \mathbf{U}_1 = \mathbf{b}_1 \otimes \mathbf{m}_1. \quad (22)$$

Right-multiplying both sides of equation (22) by $\mathbf{U}_1^{-1}$ and rearranging, equation (22) becomes

$$\mathbf{Q}_1(\mathbf{I} + \lambda\mathbf{a} \otimes \mathbf{U}_1^{-1}\mathbf{n}) = \mathbf{I} + \mathbf{b}_1 \otimes \mathbf{U}_1^{-1}\mathbf{m}_1 \quad (23)$$

which can be solved analytically as [8]:

$$\mathbf{b}_1 = \frac{1}{\sqrt{4+\lambda^2\zeta^2}}\left(-\lambda^2\zeta^2\frac{\mathbf{a}}{|\mathbf{a}|} + 2\lambda\zeta\frac{\mathbf{U}_1^{-1}\mathbf{n}}{|\mathbf{U}_1^{-1}\mathbf{n}|}\right) \quad (24)$$

$$\mathbf{m}_1 = \frac{\mathbf{U}_1}{\sqrt{4+\lambda^2\zeta^2}}\left(2\frac{\mathbf{a}}{|\mathbf{a}|} + \lambda\zeta\frac{\mathbf{U}_1^{-1}\mathbf{n}}{|\mathbf{U}_1^{-1}\mathbf{n}|}\right). \quad (25)$$

In the basis

$$\left\{\frac{\mathbf{U}_1^{-1}\mathbf{n}}{|\mathbf{U}_1^{-1}\mathbf{n}|}, \quad \frac{\mathbf{a}}{|\mathbf{a}|} \wedge \frac{\mathbf{U}_1^{-1}\mathbf{n}}{|\mathbf{U}_1^{-1}\mathbf{n}|}, \quad \frac{\mathbf{a}}{|\mathbf{a}|}\right\},$$

$$\mathbf{Q}_1 = \frac{1}{4+\lambda^2\zeta^2}\begin{bmatrix} 4-\lambda^2\zeta^2 & 0 & 4\lambda\zeta \\ 0 & 4+\lambda^2\zeta^2 & 0 \\ -4\lambda\zeta & 0 & 4-\lambda^2\zeta^2 \end{bmatrix} \quad (26)$$

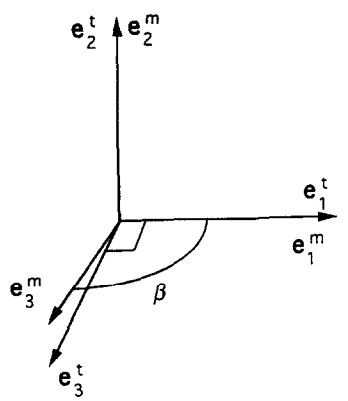

Fig. 4. Initial arrangement of the tetragonal and monoclinic bases.

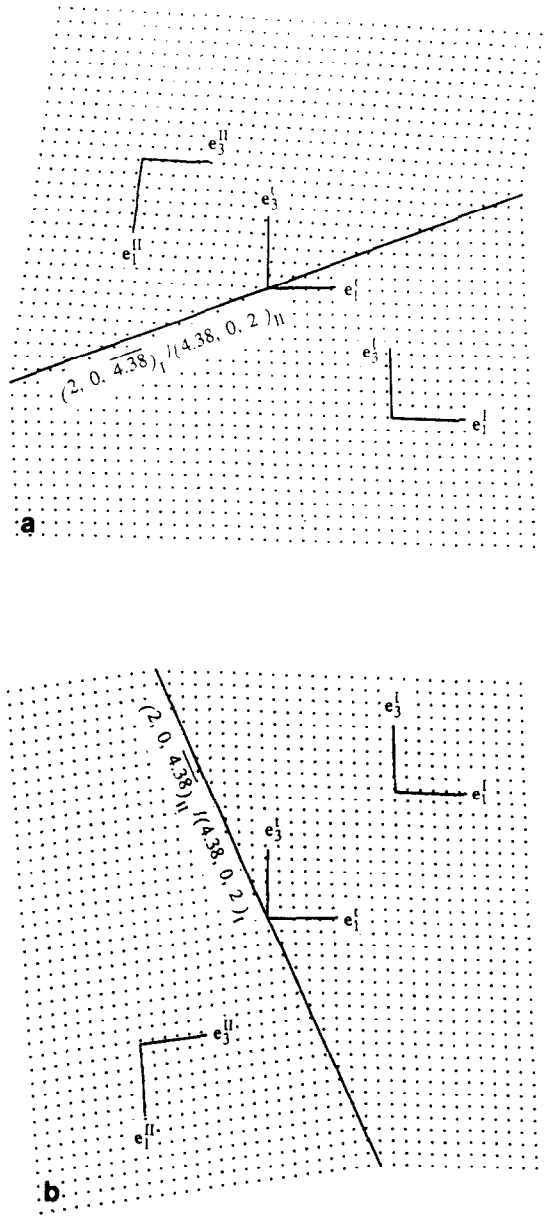

Fig. 5. Calculated domain structure in the monoclinic $LaNbO_4$ at room temperature: (a) solution 1, (b) solution 2.

where $\zeta = |\mathbf{a}||\mathbf{U}_1^{-1}\mathbf{n}|$. For the case of $\mathbf{Q}_2\mathbf{C}_i - \mathbf{U}_2 = \mathbf{b}_2 \otimes \mathbf{m}_2$, i.e.

$$\mathbf{Q}_2(\lambda\mathbf{R}\mathbf{U}_2 + (1-\lambda)\mathbf{U}_1) - \mathbf{U}_2 = \mathbf{b}_2 \otimes \mathbf{m}_2 \quad (27)$$

we have

$$\mathbf{Q}_2\mathbf{R}(\lambda\mathbf{U}_2 + (1-\lambda)\mathbf{R}^T\mathbf{U}_1) - \mathbf{U}_2 = \mathbf{b}_2 \otimes \mathbf{m}_2.$$

Let $\delta = 1 - \lambda$, then

$$\mathbf{Q}_2\mathbf{R}((1-\delta)\mathbf{U}_2 + \delta\mathbf{R}^T\mathbf{U}_1) - \mathbf{U}_2 = \mathbf{b}_2 \otimes \mathbf{m}_2. \quad (28)$$

From equation (7) we get

$$\mathbf{R}^T\mathbf{U}_1 - \mathbf{U}_2 = -\mathbf{R}^T\mathbf{a} \otimes \mathbf{n}. \quad (29)$$

Substituting equation (29) into (28)

$$\mathbf{Q}_2\mathbf{R}(\mathbf{U}_2 + \delta(-\mathbf{R}^T\mathbf{a} \otimes \mathbf{n})) - \mathbf{U}_2 = \mathbf{b}_2 \otimes \mathbf{m}_2. \quad (30)$$

Right-multiplying both sides of equation (30) by $\mathbf{U}_2^{-1}$

$$\mathbf{Q}_2\mathbf{R}(\mathbf{I} + \delta(-\mathbf{R}^T\mathbf{a} \otimes \mathbf{U}_2^{-1}\mathbf{n})) = \mathbf{I} + \mathbf{b}_2 \otimes \mathbf{U}_2^{-1}\mathbf{m}_2 \quad (31)$$

which is in the same form as equation (23), and can be solved by

$$\mathbf{b}_2 = \frac{1}{\sqrt{4 + (1-\lambda)^2\eta^2}} \left(-(1-\lambda)^2\eta^2 \frac{-\mathbf{R}^T\mathbf{a}}{|-\mathbf{R}^T\mathbf{a}|} + 2(1-\lambda)\eta \frac{\mathbf{U}_2^{-1}\mathbf{n}}{|\mathbf{U}_2^{-1}\mathbf{n}|} \right) \quad (32)$$

$$\mathbf{m}_2 = \frac{\mathbf{U}_2}{\sqrt{4 + (1-\lambda)^2\eta^2}} \left(2\frac{-\mathbf{R}^T\mathbf{a}}{|-\mathbf{R}^T\mathbf{a}|} + (1-\lambda)\eta \frac{\mathbf{U}_2^{-1}\mathbf{n}}{|\mathbf{U}_2^{-1}\mathbf{n}|} \right). \quad (33)$$

In the basis

$$\left\{ \frac{\mathbf{U}_2^{-1}\mathbf{n}}{|\mathbf{U}_2^{-1}\mathbf{n}|}, \frac{-\mathbf{R}^T\mathbf{a}}{|-\mathbf{R}^T\mathbf{a}|} \wedge \frac{\mathbf{U}_2^{-1}\mathbf{n}}{|\mathbf{U}_2^{-1}\mathbf{n}|}, \frac{-\mathbf{R}^T\mathbf{a}}{|-\mathbf{R}^T\mathbf{a}|} \right\}$$

$$\mathbf{Q}_2\mathbf{R} = \frac{1}{4 + (1-\lambda)^2\eta^2} \begin{bmatrix} 4 - (1-\lambda)^2\eta^2 & 0 & 4(1-\lambda)\eta \\ 0 & 4 + (1-\lambda)^2\eta^2 & 0 \\ -4(1-\lambda)\eta & 0 & 4 - (1-\lambda)^2\eta^2 \end{bmatrix} \quad (34)$$

where $\eta = |-\mathbf{R}^T\mathbf{a}||\mathbf{U}_2^{-1}\mathbf{n}|$, and $\delta = 1 - \lambda$ has been applied. Thus the average laminate/domain interface for both cases, $\mathbf{m}_1$ and $\mathbf{m}_2$, is obtained. The angle between the domain boundary and the laminate/domain interface in the deformed configuration, ϕ, can be calculated by

$$\phi_i = \cos^{-1}\left(\frac{\mathbf{U}_i^{-1}\mathbf{m}_i \cdot (\mathbf{Q}_i\mathbf{U}_i)^{-T}\mathbf{n}}{|\mathbf{U}_i^{-1}\mathbf{m}_i||(\mathbf{Q}_i\mathbf{U}_i)^{-T}\mathbf{n}|} \right). \quad (35)$$

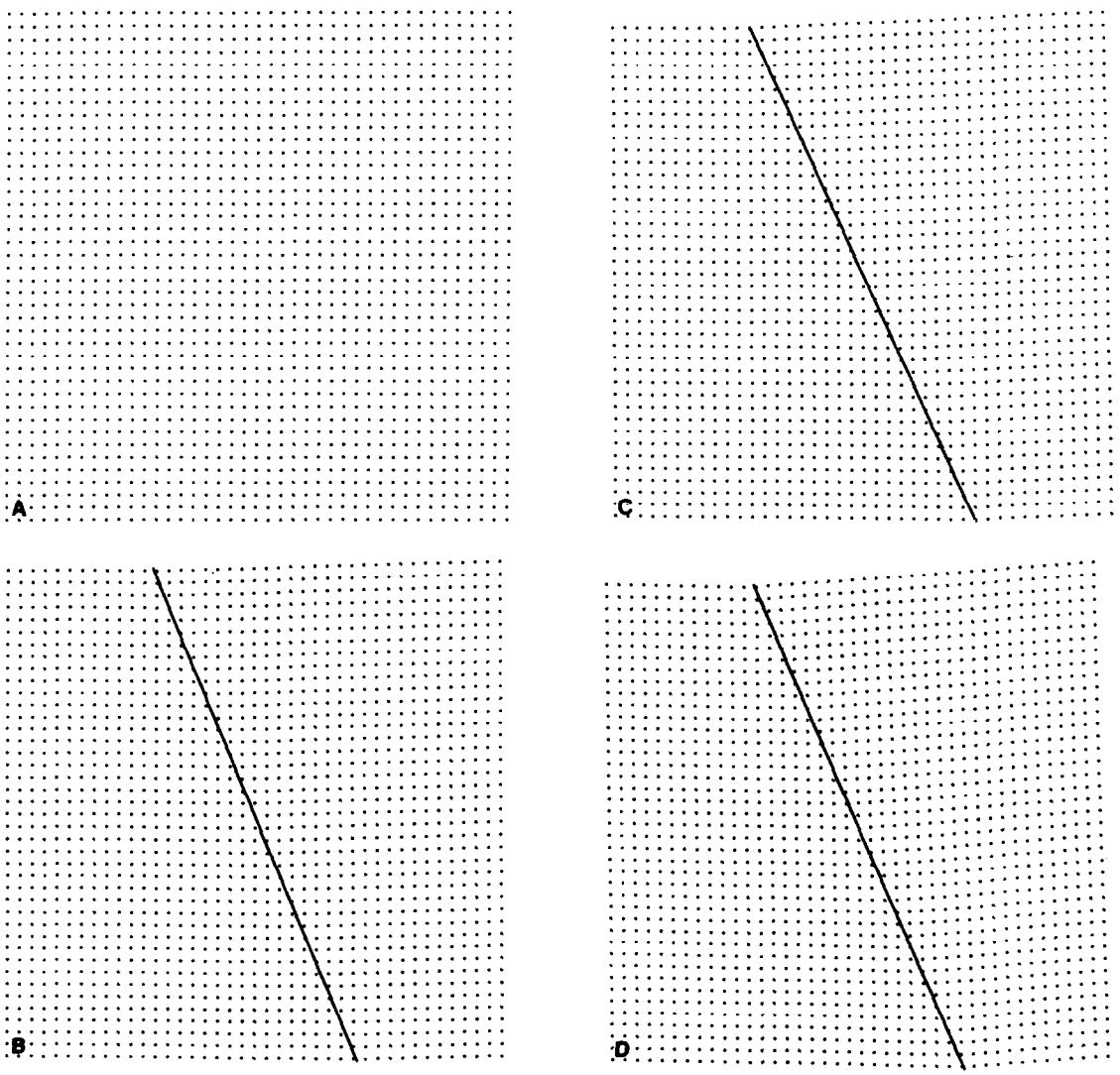

Fig. 6(a)–(d) *Caption overleaf.*

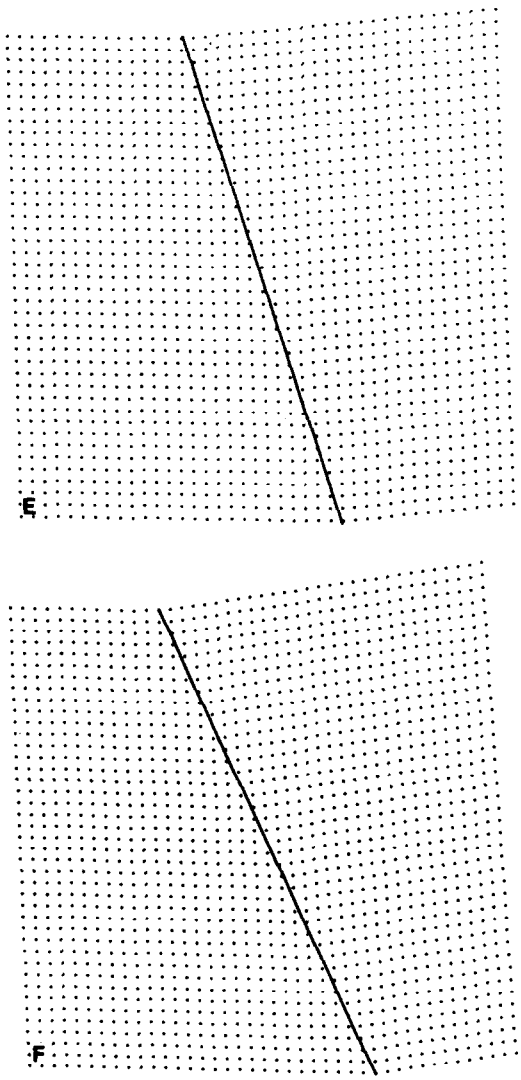

Fig. 6. Evolution of domain structure with temperature: (a) 520°C (undeformed), (b) 500°C, (c) 480°C, (d) 400°C, (e) 300°C, and (f) room temperature.

It is noted that there are two solutions for equation (7), therefore $\mathbf{m}_1$ and $\mathbf{m}_2$ have two crystallographically equivalent solutions, respectively. All these solutions are functions of the volume fraction λ.

3. APPLICATION TO $LaNbO_4$

Table 1 shows the lattice parameters at various temperatures for both the tetragonal phase and the monoclinic phase in $LaNbO_4$ [5]. The transformation temperature is near 520°C. Initially setting the tetragonal and monoclinic lattice vectors as shown in Fig. 4, we have

$$\mathbf{e}_i^m = \mathbf{U}\mathbf{e}_i^t,$$

where

$$\mathbf{U} = \begin{bmatrix} \alpha & 0 & \sin\beta \\ 0 & \delta & 0 \\ 0 & 0 & \cos\beta \end{bmatrix}$$

Table 2. $\mathbf{m}_i$ and ϕ_i as a function of λ

λ	0.25	0.50	0.75
$\mathbf{m}_1^{(1)}$	(−0.9541, 0, −0.2995)	(−0.9464, 0, −0.3230)	(−0.9381, 0, 0.3464)
$\mathbf{m}_1^{(2)}$	(−0.4376, 0, 0.8992)	(−0.4152, 0, 0.9097)	(−0.3295, 0, 0.9198)
$\mathbf{m}_2^{(1)}$	(0.9198, 0, 0.3295)	(0.9097, 0, 0.4152)	(0.8992, 0, 0.4376)
$\mathbf{m}_2^{(2)}$	(0.3464, 0, −0.9381)	(0.3230, 0, −0.9464)	(0.2995, 0, −0.9541)
ϕ_1, degree	91.43	92.86	94.28
ϕ_2, degree	94.28	92.86	91.43

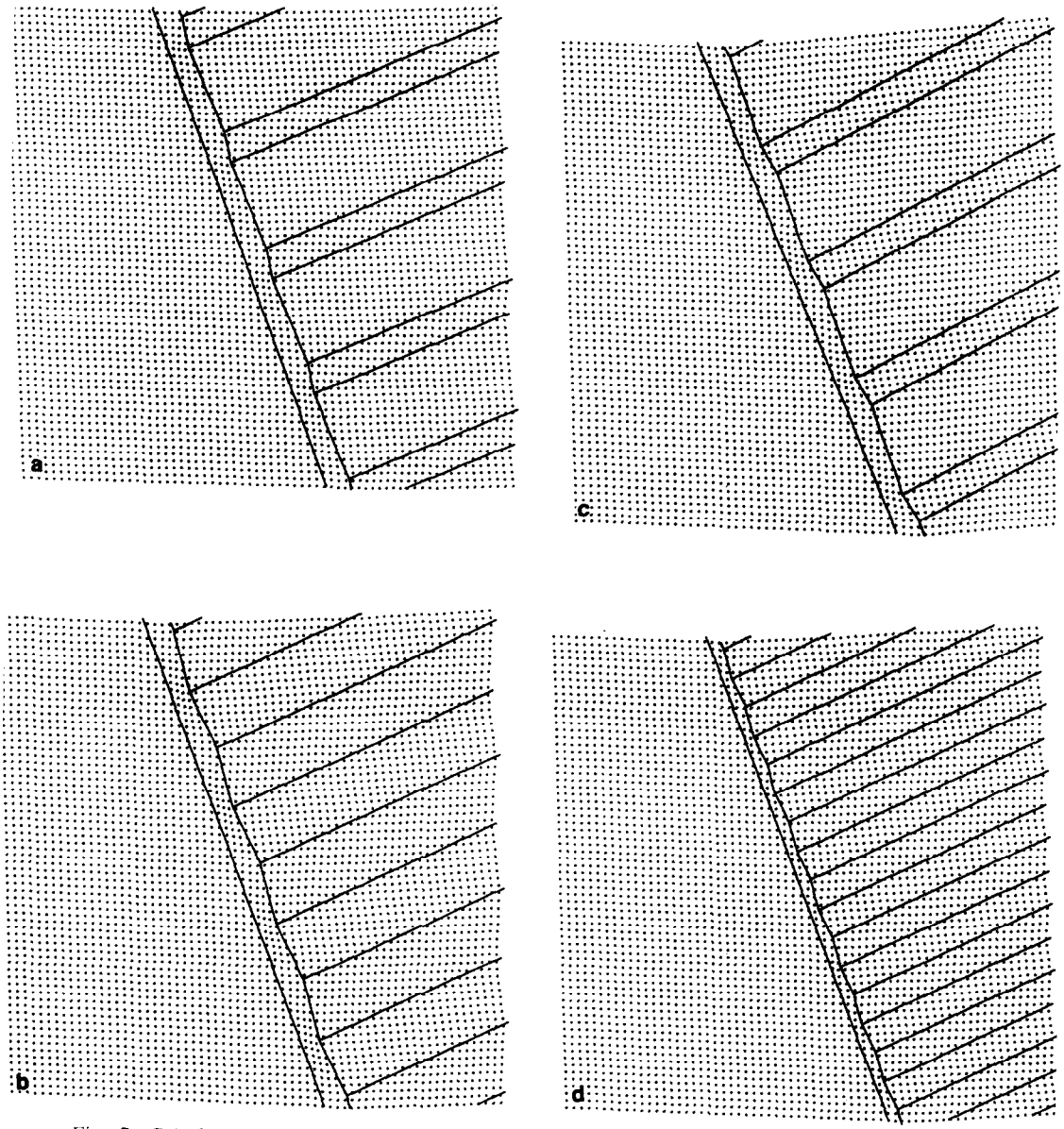

Fig. 7. Calculated laminate/domain structure in the monoclinic $LaNbO_4$ (from the solution of $\mathbf{Q}(\mathbf{U}_1 + \lambda \mathbf{a}_1 \otimes \mathbf{n}_1) - \mathbf{U}_1 = \mathbf{b}_1 \otimes \mathbf{m}_1$): (a) $k = 10$, $\lambda = 0.25$, (b) $k = 10$, $\lambda = 0.5$, (c) $k = 10$, $\lambda = 0.75$, (d) $k = 20$, $\lambda = 0.5$.

and

$$\alpha = \frac{e_1^m}{e_1^t} = \frac{5.633}{5.450} = 1.03358, \quad \delta = \frac{e_2^m}{e_2^t} = \frac{11.666}{11.80}$$

$$= 0.98864, \quad \gamma = \frac{e_3^m}{e_3^t} = \frac{5.261}{5.450} = 0.96532$$

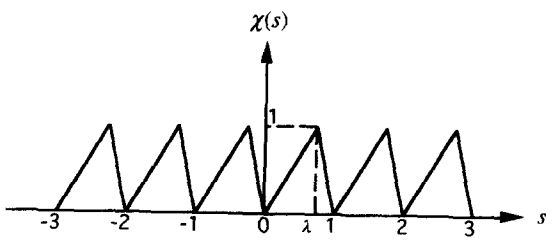

Fig. 8. Definition of $\chi(s)$ function.

and β, the monoclinic angle, is 94.15° at room temperature. Symmetrizing $\mathbf{U}$ by using the polar decomposition, we get, at room temperature,

$$\mathbf{U}_1 = \begin{bmatrix} 1{,}03295 & 0 & -0.03615 \\ 0 & 0{,}98864 & 0 \\ -0.03615 & 0 & 0.96464 \end{bmatrix},$$

and following equation (5)

$$\mathbf{U}_2 = \begin{bmatrix} 0{,}96464 & 0 & 0{,}03615 \\ 0 & 0{,}98864 & 0 \\ 0.03615 & 0 & 1.03295 \end{bmatrix}.$$

Now, all the calculations of Section 2 can be carried out for $LaNbO_4$. The eigenvalues of $\mathbf{U}_1^{-1}\mathbf{U}_2^2\mathbf{U}_1^{-1}$ are $\lambda_1 = 0.81929$, $\lambda_2 = 1$, and $\lambda_3 = 1.22056$, satisfying the condition of $\lambda_2 = 1$. The corresponding eigenvectors

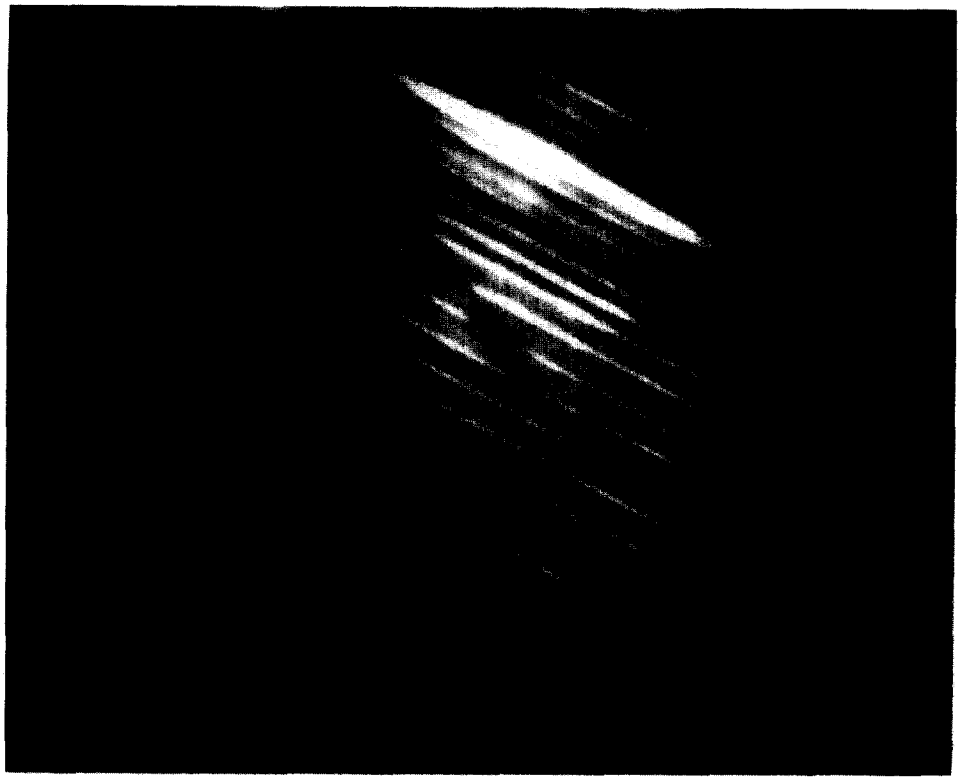

Fig. 9. TEM microstructure of the monoclinic $LaNbO_4$ at room temperature. Bright Field.

are $\mathbf{e}_1 = (-0.91836, 0, 0.39575)$, $\mathbf{e}_2 = (0, 1, 0)$, and $\mathbf{e}_3 = (-0.39575, 0, -0.91836)$. Substituting λ_1, λ_3, $\mathbf{e}_1$, and $\mathbf{e}_3$ into equations (9) and (10), two solutions are obtained:

$$\mathbf{n}_1 = [0.07341, 0, -0.18460]$$

$$\mathbf{a}_1 = [-0.94644, 0, 0.32288]$$

and

$$\mathbf{n}_2 = [0.18460, 0, 0.07341]$$

$$\mathbf{a}_2 = [-0.41529, 0, -0.90968].$$

The corresponding deformed normals are

$$\mathbf{n}_1' = [0.06446, 0, -0.18895]$$

$$\mathbf{n}_2' = [0.18161, 0, 0.08291].$$

Consequently, two rotation matrices $\mathbf{R}^{(1)}$ and $\mathbf{R}^{(2)}$ are obtained according to equation (11):

$$\mathbf{R}^{(1)} = \begin{bmatrix} 0,99506 & 0 & 0,09933 \\ 0 & 1 & \\ -0.09933 & 0 & 0.99506 \end{bmatrix}$$

$$\mathbf{R}^{(2)} = \begin{bmatrix} 0.99506 & 0 & -0.09933 \\ 0 & 1 & 0 \\ 0.09933 & 0 & 0.99506 \end{bmatrix}$$

as illustrated in Fig. 2(b). They are 5.7° and −5.7° rotations, respectively, about the $\mathbf{e}_2^m$ axis. The orientation relationship is predicted to be,

$$\mathbf{R}^{(1)}\mathbf{R}_s = \begin{bmatrix} -0.09933 & 0 & 0,99506 \\ 0 & 1 & 0 \\ -0.99506 & 0 & -0.09933 \end{bmatrix}$$

or

$$\mathbf{R}^{(2)}\mathbf{R}_s = \begin{bmatrix} 0,09933 & 0 & 0,99506 \\ 0 & 1 & 0 \\ -0.99506 & 0 & -0.09933 \end{bmatrix}$$

corresponding to a 95.7° or a 84.3° rotation about the $\mathbf{e}_2^m$ axis. Figure 5 graphically shows the calculated results of the two solutions at room temperature. To obtain Fig. 5, a grid of dots was plotted, representing the reference configuration viewed along the $\mathbf{e}_2^t$ axis. The deformed position of each dot was calculated by applying the deformation $\mathbf{y}(\mathbf{x}) = \mathbf{R}^{(k)}\mathbf{U}_2\mathbf{x}$ for $\mathbf{x}\cdot\mathbf{n}_k > 0$ and $\mathbf{y}(\mathbf{x}) = \mathbf{U}_1\mathbf{x}$ for $\mathbf{x}\cdot\mathbf{n}_k \leqslant 0$ to each dot, $k = 1, 2$, corresponding to solutions 1 and 2. Since the monoclinic lattice possesses a two-fold rotation symmetry about $\mathbf{e}_2^m$, the two solutions show the same lattice orientation relationship between the two domains. The index of the domain boundary with

respect to the monoclinic bases $\mathbf{e}_j^{m_I}$ and $\mathbf{e}_j^{m_{II}}$, converted from the index of the normal to the boundary with respect to the reference basis, is $(2, 0, \overline{4.38})_{m_I}$, $(4.38, \underline{0}, 2)_{m_{II}}$ for solution 1 and $(4.38, 0, 2)_{m_I}$, $(2, 0, \overline{4.38})_{m_{II}}$ for solution 2. If we exchange the subscripts I and II in solution 2, the index of the boundary is then consistent with that in solution 1. Notice that the orientation relationship shown in Fig. 5 represents neither a Type I nor a Type II twin [10, 11].

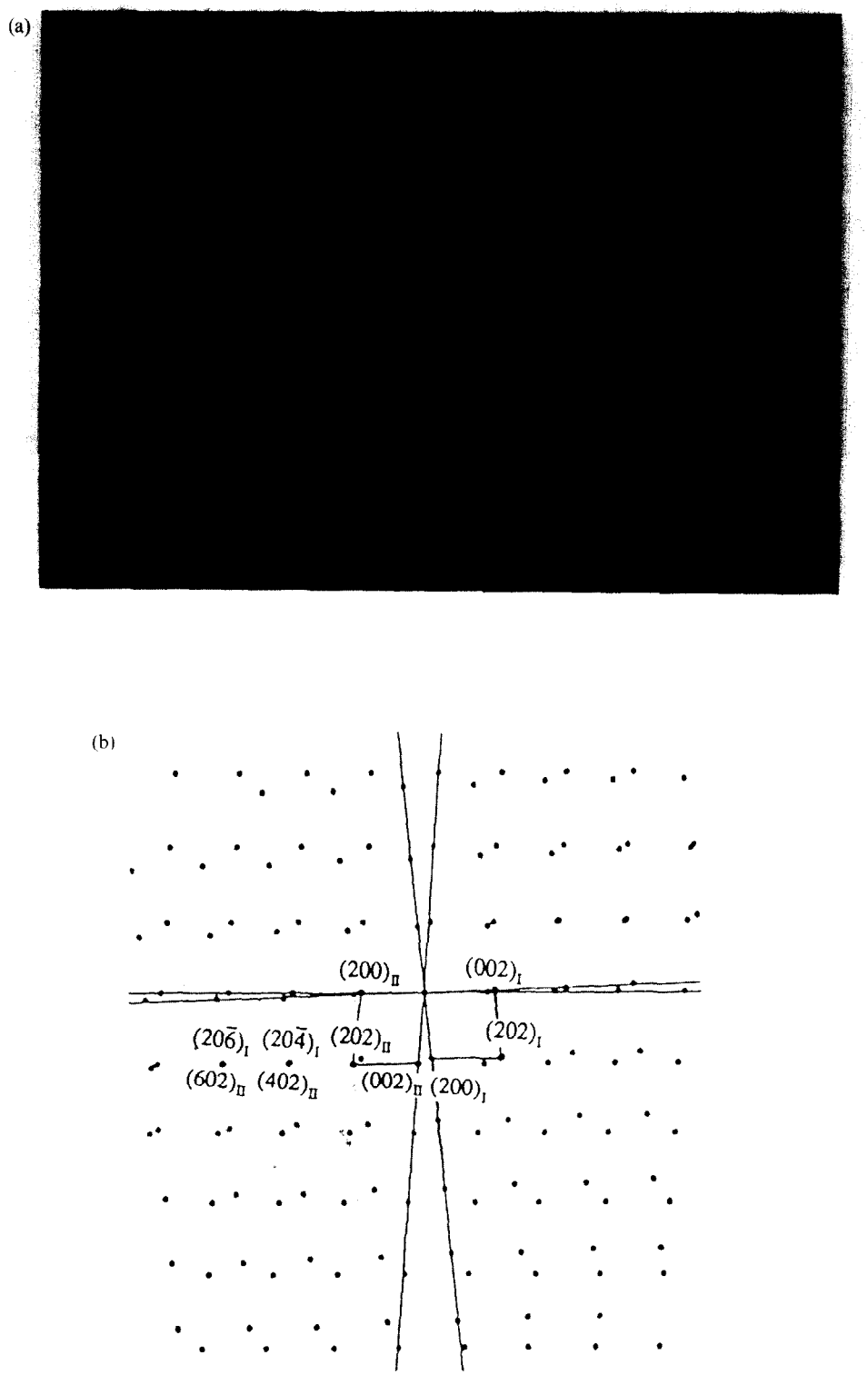

Fig. 10. (a) TEM selected area diffraction pattern corresponding to Fig. 9. (b) Index of the pattern, showing two sets of diffraction spots from two orientations with the same zone axis [010].

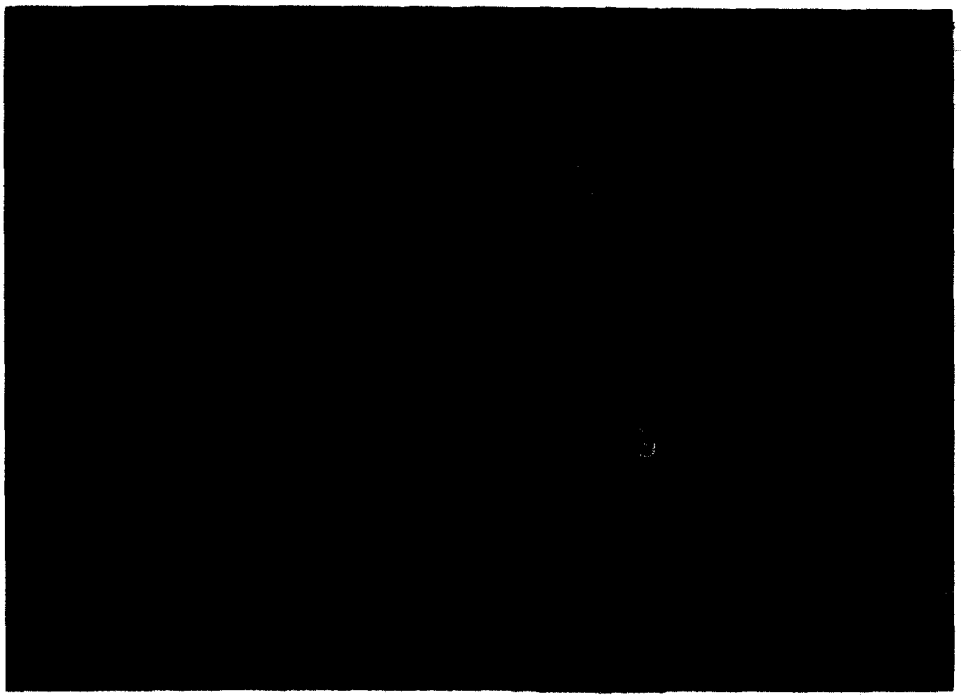

Fig. 11. Optical microstructure of the monoclinic $LaNbO_4$, showing the laminate/domain structure.

In a similar way, the domain structure at temperatures above room temperature can be predicted by using the lattice parameter data listed in Table 1. Some of them are illustrated in Fig. 6, demonstrating the evolution of the monoclinic structure with temperature.

By equations (25) and (33), the index of the average laminate/domain interface can be calculated numerically as a function of λ, and following equation (35), the angle between the domain boundary and the laminate/domain interface can be evaluated. These results are listed in Table 2. Note that the normal to the laminate/single domain interface changes only a little with volume fraction. Figure 7 shows the calculated laminate/domain structures, including the change in the interface orientation with λ, and the change in the width of the intermediate layer with k. To obtain these graphs, the deformation

$$\mathbf{y}_i^k(\mathbf{x}) = \mathbf{Q}_i(\lambda\mathbf{R}\mathbf{U}_2 + (1-\lambda)\mathbf{U}_1)\mathbf{x} + \frac{1}{k}\chi(k\mathbf{x}\cdot\mathbf{n})\mathbf{Q}_i\mathbf{a} \quad (36)$$

is applied to the grid of dots on $\mathbf{x}\cdot\mathbf{m}_i < 0$, where χ is a function defined by Fig. 8. For $\mathbf{x}\cdot\mathbf{m}_i \geqslant 1/k$, the deformation is

$$\mathbf{f}_i^k(\mathbf{x}) = \mathbf{U}_i\mathbf{x} \quad (37)$$

and in the intermediate region, $0 \leqslant \mathbf{x}\cdot\mathbf{m}_i < 1/k$, the deformation is chosen as

$$\mathbf{g}_i^k(\mathbf{x}) = \xi^{(k)}(\mathbf{x}\cdot\mathbf{m})\mathbf{f}_i^k(\mathbf{x}) + (1-\xi^{(k)}(\mathbf{x}\cdot\mathbf{m}))\mathbf{y}_i^k(\mathbf{x}) \quad (38)$$

where $\xi^{(k)}$ can be any function with the property that $\xi^{(k)} = 0$ for $\mathbf{x}\cdot\mathbf{m} = 0$, and $\xi^{(k)} = 1$ for $\mathbf{x}\cdot\mathbf{m} = 1/k$, so that $\mathbf{g}_i^k(\mathbf{x})$ is compatible with both sides of the intermediate region [1]. In the current calculation,

$$\xi^{(k)}(\mathbf{x}\cdot\mathbf{m}) = \tfrac{1}{2}(\sin(k\mathbf{x}\cdot\mathbf{m} - 0.5)\pi + 1) \quad (39)$$

is selected for convenience. Note that equation (36) simply alternates the solution found earlier for the simple domains on layers with volume fraction λ.

4. EXPERIMENTAL EVIDENCE [5–7]

Figure 9 is a typical TEM room temperature micrograph of the monoclinic $LaNbO_4$ crystals, showing the domains. Figure 10(a) is the TEM selected area diffraction pattern corresponding to Fig. 9. In this diffraction pattern, there are two sets of diffraction spots, each of them originating from one of the two orientations of domain. The zone axis for both sets of spot is the [010] direction of the monoclinic lattice which is parallel to the four-fold axis of the parent tetragonal lattice. The index of the pattern is shown in Fig. 10(b), which indicates that the orientation relationship between these two adjacent monoclinic lattices is a rotation of near 95.6° about the [010] axis. This result matches that predicted by the Ball–James theory (Section 3). Examining the diffraction pattern carefully, we can find that almost every diffraction spot from one orientation is separated from that of another orientation except the spots $(20\bar{6})_{\mathrm{I}}/(602)_{\mathrm{II}}$ and $(20\bar{4})_{\mathrm{I}}/(402)_{\mathrm{II}}$. This implies that $(20\bar{6})_{\mathrm{I}}/(602)_{\mathrm{II}}$ or $(20\bar{4})_{\mathrm{I}}/(402)_{\mathrm{II}}$ are almost parallel to each other with near interplanar spacing, and the domain boundary must lie in between $(20\bar{6})_{\mathrm{I}}/(602)_{\mathrm{II}}$ and $(20\bar{4})_{\mathrm{I}}/(402)_{\mathrm{II}}$ planes with a irrational Miller index. The predicted domain boundary lies in $(2, 0, 4.38)_{\mathrm{I}}/(4.38, 0, 2)_{\mathrm{II}}$.

Figure 11 is an optical microscope picture of the monoclinic $LaNbO_4$ with the specimen surface

normal parallel to the $\mathbf{e}_2^m$, showing an example of the laminate/domain structure. The volume fraction λ in the laminate region is estimated near 0.5. The angle between the interface and the domain boundary is measured as 92 degrees, which is in very good agreement with the calculated value for $\lambda = 0.5$.

Acknowledgements—The authors thank AFOSR (F49620-97-1-0187), ONR/DARPA (N00014-95-1-1145) and NSF (DMS-9505077) for supporting this work.

REFERENCES

1. Ball, J. M. and James, R. D., *Phil. Trans. R. Soc. Lond.*, 1992, **A338,** 389.
2. James, R. D., *MRS Symp.*, 1992, **246,** 81.
3. Ball, J. M. and James, R. D., Theory for the microstructure of martensite and applications. *ICOMAT'92*, ed. C. M. Wayman and J. Perkins. Monterey Institute for Advanced Studies, Carmel, 1993, p. 65.
4. Chu, C. and James, R. D., Analysis of microstructures in Cu–14.0%Al–3.9%Ni by energy minimization. *ICOMAT'95, J. de Physique IV*, Colloque C8, Vol. 5, 1995, p. 143.
5. Jian, Li, Domain structure, phase transformation, mechanical behavior and share memory effect in rate earth orthoniobate $LaNbO_4$. Ph.D. thesis, University of Illinois at Urbana-Champaign, 1995.
6. Jian, Li and Wayman, C. M., *J. Am. Ceram. Soc.*, 1997, **80,** 803.
7. Jian, Li and Wayman, C. M., *J. Am. Ceram. Soc.*, 1996, **79,** 1642.
8. Chu, C.-H., Hysteresis and microstructures: a study of biaxial loading on compound twins of copper–aluminium–nickel single crystals. Ph.D. thesis, University of Minnesota, 1993.
9. Aizu, K., *J. Phys. Soc. Jap.*, 1970, **28,** 706.
10. Li Jian and Wayman, C. M., *Acta metall. mater.*, 1995, **43,** 3893.
11. Simha, N. K., *J. Mech. Phys. Solids*, 1997, **45,** 261.